Characterising and control of ammonia emission in microbial fuel cells

Dunzhu Li[a,1], *Yunhong Shi*[a,1], *Fei Gao*[a], *Luming Yang*[a], *Daniel K. Kehoe*[b], *Luis Romeral*[b,c], *Yurii K. Gun'ko*[c,d], *Michael G. Lyons*[b,c], *Jing Jing Wang*[b], *Daragh Mullarkey*[b], *Igor V. Shvets*[b], *Liwen Xiao*[a,e,*]

[a]Department of Civil, Structural and Environmental Engineering, Trinity College Dublin, Dublin 2, Ireland.

[b]AMBER Research Centre and Centre for Research on Adaptive Nanostructures and Nanodevices (CRANN), Trinity College Dublin, D2, Ireland

[c]School of Chemistry, Trinity College Dublin, Dublin 2, Ireland

[d]BEACON, Bioeconomy SFI Research Centre, University College Dublin, Dublin 4, Ireland

[e]TrinityHaus, Trinity College Dublin, Dublin 2, Ireland

*Corresponding author. Telephone: +3531896 3741. Email: liwen.xiao@tcd.ie

[1] Dunzhu Li and Yunhong Shi contribute equally to this work

ABSTRACT

The serious ammonia (NH_3) emission of air-cathode microbial fuel cells (MFCs) was reported but how to control and mitigate the emission hasn't been well studied. Considering the importance of the issue for the application of MFCs in wastewater treatment, this study

foused on understanding the NH_3 emission process in MFCs and investigating mitigation approaches. The study found that when feeding with dairy wastewater the typical flat-cathode MFCs can emitt NH_3 of more than 0.82 mg-N/L. The NH_3 emission reduced with the grown of cathode biofilm and the decrease of ammonium concentration in the influent. Combined experimental and theoretical results showed that the current density rather than the total current was the determined factor for ammonia emission. The novel Cu-blended 3D cathode developed in this study significantly decreased the NH_3 emission to 0.037 mg-N/L (or 0.068% of the total removed ammonium), which was 6.3% of that in the activated sludge wastewater treatment plants (WWTP). In addition, the good power performance and high pollutants removal (14.4 W/m^3, 88.1%-COD and 92.8%-TN removal) were also obtained by the Cu-blended 3D cathodes. This study unveiled the ammonia emission process and proposed effective mitigation methods, which will promote the practical application of MFCs for ammonium-rich wastewater treatment.

Keywords: microbial fuel cells; NH_3 emission; 3D cathodes; Cu-blended

Graphical abstract

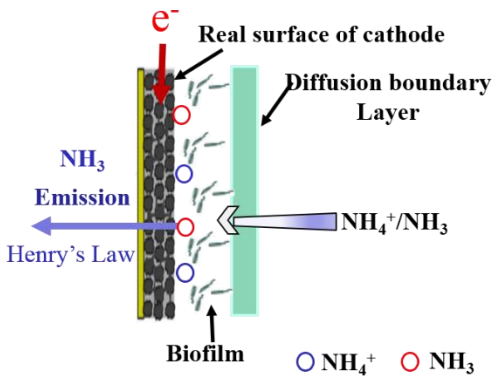

1. Introduction

Gaseous ammonia (NH_3) is one of the air pollutants which could cause many environmental issues such as visibility degradation, greenhouse effect and acid deposition [1, 2]. More importantly, it is a critical chemicals involved in the secondary aerosol formation, which increases the concentration of fine particulate (PM2.5) in the air [3] and poses great risk to the public health. In fact, NH_3 is considered as a key to limit deadly haze episodes [4]. In Salt Lake City, it was reported that three quarters of the fine particles in the winter haze were made up of ammonium nitrate, which was formed when the NH_3 combined with nitrogen oxides [4]. In China, it was found that the emission of NH_3 had a strong link with the PM2.5 levels and reduction of NH_3 emission could help mitigate PM2.5 pollution [5]. NH_3 emissions are increasing and the main emission sources include agricultural activities, industrial processes, fuel burning and waste and wastewater managements [6]. Although the NH_3 emission only accounted for around 1% of the total ammonium removal, traditional wastewater treatment plants (WWTPs) are the fifth biggest contributor of NH_3 [2], with the emission factors of between 0.15 to 0.29 mg NH_3/L sewage[2]. To reduce the NH_3 emission, US recommended the emission factor for WWTPs of between 0.02 to 0.003 mg NH_3/L sewage [7], while in China the emission factors of 0.003 mg NH_3/L sewage or lower were suggested [2].

Microbial fuel cells (MFCs) are promising approaches for recovering the energy and removing pollutants from wastewater [8-11]. When MFCs was used to treat ammonium-abundant wastewater such as swine wastewater, dairy wastewater and animal slurry, up to 95% of the total nitrogen (TN) could be removed [9, 12-15]. While the TN removal in the

MFCs could be due to biological processes such as nitrification/denitrification [9, 15-18], many studies suggested that ammonia volatilization could also played an important role [12, 19, 20]. It was found that during the electricity generation, the pH near the cathode increases which accelerates the conversion of ammonium ion (NH_4^+) to free ammonia (FA) [12, 20]. FA could volatise through the cathodes. In their study, Kim et al suggested that NH_3 emission contributed to around 60% of the ammonia removal in their MFCs [12]. Due to the potential high NH_3 emission, MFC technologies have been successfully used to recover NH_3 from nitrogen rich wastewater such as urine [19, 21-23]. High NH_3 emission could seriously undermine the application of MFCs for wastewater treatment, considering the importance of NH_3 in fighting climate change and air pollution. Therefore, to facilitate the application of MFCs for wastewater treatments, an in-depth understanding of ammonium removal and NH_3 emission mechanisms in MFCs is very necessary.

The high total current was considered as one of the major factors for NH_3 emission of MFCs [12, 19]. During the electricity generation, protons loss near the cathode results in a localized high pH [12], where ammonium is converted to NH_3. Therefore, lowering the current generation would be a convenient way to reduce NH_3 production. However, the current and power generation of MFCs is considered relatively low and lots of efforts have been made to increase the current generation for practical application of MFCs [24]. This leads to a dilemma for MFC development. Effective methods to mitigate NH_3 emission are needed when improving the current generation of MFCs for practical application.

In this study, a novel 3D Cu-blended cathode – which could significantly increase cathode specific surface area (CSSA) - was proposed to reduce the NH_3 emission and improve the

current generation. This study first investigated the NH_3 emission process and mechanism from typical MFCs, and then assessed the performance of the 3D cathodes with and without Cu on mitigating NH_3 emission and improving power generation. Multiple electrode analysis methods, including scanning electron microscope (SEM), energy dispersive X-ray (EDX) as well as atomic force microscope (AFM) were used to characterize the Cu-blended 3D cathode before and after the experiments. The results reported not only reveal the NH_3 emission mechanism but also supply a novel method to effectively control the emission as well as improve power performance.

2. Methods and materials

2.1. MFC construction

Three types of cathode were used in this study: the typical flat cathodes, the 3D cathodes and Cu-blended 3D cathode. The typical flat cathode was made as previous described [25]. Stainless steel mesh (60 × 60, type 304, Belleville wire cloth, USA) was projected by a mixture of activated carbon (300 mg, AC, Norit SX plus, Cabot Corporation, USA), carbon black (30 mg, CB, Vulcan XC-72, Cabot Corporation, USA) and 1 mL poly (vinylidene fluoride, PVDF, Sigma Aldrich). One layer of glass microfiber filter (CAT No. 1822-047, Waterman) was placed on the cathode surface (solution side) as a separator. The 3D cathode was made of cylindrical stainless steel mesh (90 mm in length and 16 mm in diameter, mesh size 0.6 mm, type 304, Aliexpress) which was projected by the mixture using the same material as typical flat cathode (900 mg activated carbon, 90 mg carbon black and 3 mL PVDF; real working area of 28.3 cm^2) and wrapped by one layer of separator. The Cu-

blended 3D cathode was made following the same procedure as the 3D cathode, except that the CB in the mixture was replaced by Cu particles: In the mixture, 450 mg Cu-particles (10-40 mesh, Sigma-Aldrich) was blended with 900 mg AC and 3 mL PVDF. The mixture was projected into the surface of cylindrical stainless steel mesh (first 60 mm part of the 90 mm long cylinder mesh, real working area of 28.3 cm^2, Fig. 1). After carefully smoothed the surface, the cathodes were soaked into deionized (DI) water for 15 minutes and then air-dried for 8 hours before assembly.

Table 1
Details of MFCs used in the test

Abbreviation	Configuration description	Cathode Area (cm^2)	Net volume (mL)	Cathode specific Surface area (m^2/m^3)
1Flat	1 brush anode, 1 flat cathode	7	20	35.0
CSA1C	1 cylindrical cathode surrounding anode	28.3	230	12.3
CSA2C	2 cylindrical cathodes surrounding anode	56.5	230	24.6
CSACu1C	1 Cu-blended cylindrical cathode surrounding anode	28.3	230	12.3
CSACu2C	2 Cu-blended cylindrical cathodes surrounding anode	56.5	230	24.6
CSACu4C	4 Cu-blended cylindrical cathodes surrounding anode	113	250	45.2

All the cathodes were assembled with the same type of graphite fiber brush (GFB) anode (30 mm in both diameter and length, activated by heat-treated at 450 ºC for 30 min. The flat cathode was assembled with anode in single cubic chamber (labelled as 1Flat) and the anodes were horizontally placed in the middle of the chambers of MFCs. As to the 3D cathode, the anodes were horizontally placed in the middle of the chambers and surrounded by the 3D cathodes (cathodes surrounding the anode - CSA configuration). 1 to 4 cathodes were used in this study (Table 1). Fig. 1 showed CSA with 4 cathodes. In terms of the CSA-MFCs

employed with Cu-blended cylindrical cathode, they were labeled as CSACu. In this study, MFCs of CSACu with 1C, 2C and 4C (labeled as CSACu1C, CSACu2C and CSACu4C, respectively) were assembled and used at the experiment. The details of all MFCs are showed in Table 1 and Fig. 1.

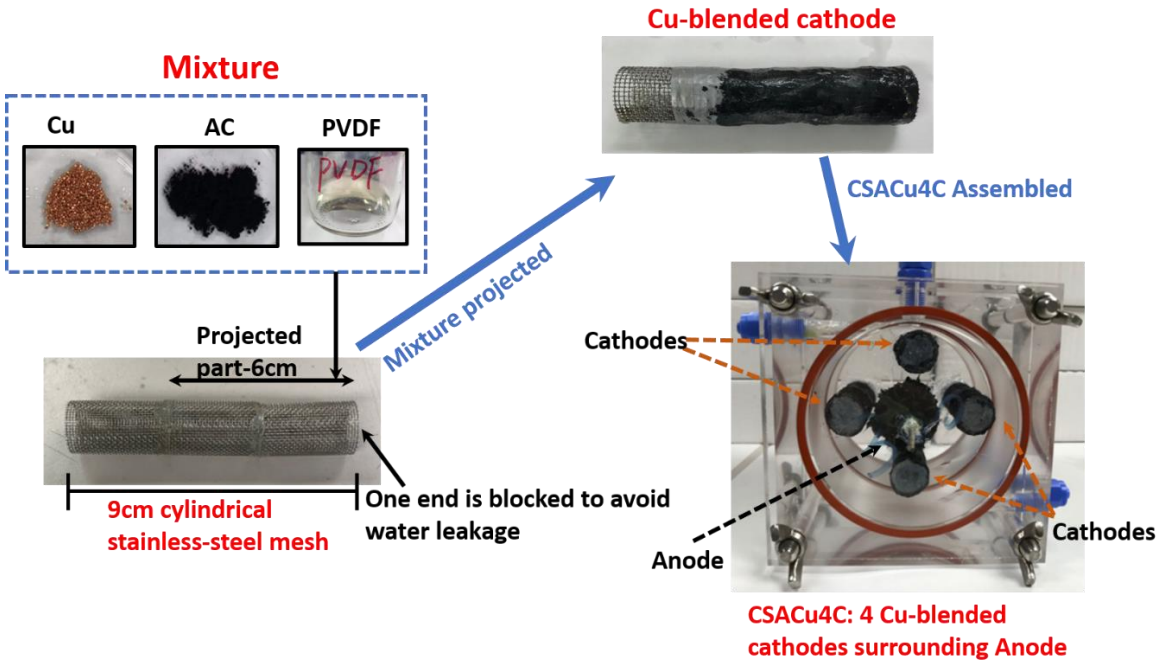

Fig. 1. The making process of Cu-blended cylindrical cathode and the assembled CSACu4C with 4 Cu-blended cathodes.

2.2. Operating conditions.

All the GFB anodes were firstly acclimated by wastewater in room temperature over 6 months (22 ± 2 °C, except as noted). Then the mature GFBs were assembled with different types of cathodes. In this study, real dairy wastewater (collected from Aurivo Dairy Ingredients, Ireland; filtered by 1 mm stainless steel mesh) was used except in the nitrogen

removal pathway study. To keep the influent stability and comparable, the dairy wastewater was diluted to the concentration of 600 ± 161 mg COD/L and 70 ± 15 mg NH_4^+-N/L before use, except as noted. To assess the impact of cathode biofilm on NH_3 emission, cathodes with mature biofilm in 1Flat MFC were replaced by new cathodes (without biofilm) after 4-month operation with diluted dairy wastewater. 1Flat MFCs were also used to study the impact of currents and influent ammonium concentrations on NH_3 emission.

CSA1C and CSA2C were used to assess the impact of 3D cathodes on NH_3 emission. MFCs with Cu-blended cathodes (CSA configuration), fueled with dairy wastewater, were developed and operated to assess the performance of Cu-blended 3D cathodes on power generation, nitrogen removal and NH_3 emission. To investigate the long-term performance of Cu-blended cathode on nitrogen removal and NH_3 emission, two identical MFCs of CSACu4C feeding with diluted dairy wastewater were operated for 14 months. To assess the power generation of Cu-blended cathode, another 2 identical CSACu4C reactors were assemblied and fed with raw dairy wastewater. To make the results comparable to previous reports [26-28], the influent was added with phosphate-buffered saline (PBS) and the operation temperature was 30 °C.

In the nitrogen removal pathway study, 2 identical 1Flat MFCs (with cathode biofilm) were operated with synthetic wastewater (1 g/L sodium acetate dissolved with 60 mg-N/L of NH_4Cl, 5 mL/L vitamins and 12.5 mL/L minerals) for 1 week. Then the synthetic wastewater mixing with nitrite-oxidizing bacteria (NOB) selective inhibitor (60 mg-S/L $Na_2S•xH_2O$) was added in the MFCs. The NH_3 emission and nitrogen concentrations in MFCs were measured before and after $Na_2S•xH_2O$ were added.

Two extra air chamber were made to collect the NH_3 emited from the 1Flat-MFCs and CSA-MFCs, respectively (Fig. 2 and Fig. S2). The air tightness of the air chambers was tested by soaking them into the water, running air pump and conducting bubble test. The test confirmed that they were air tight and could effectively collect the emitted NH_3 of MFCs.

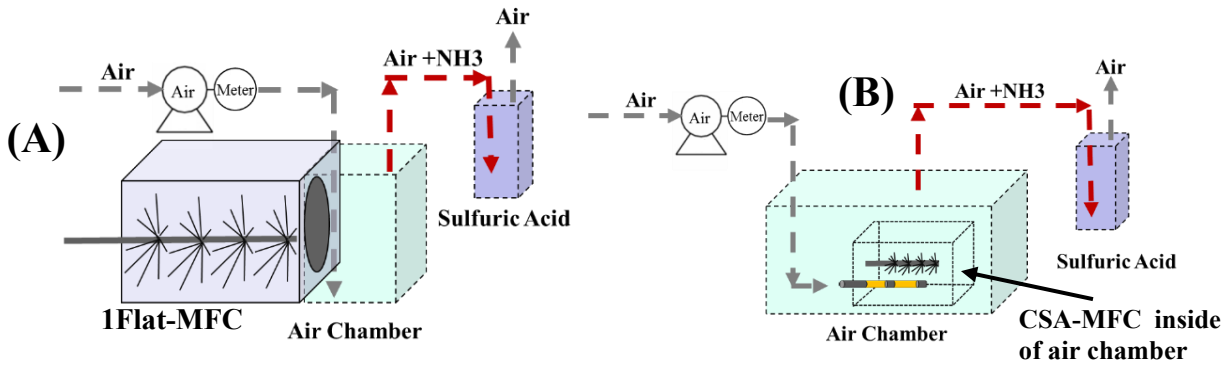

Fig. 2. Schematic diagrams of NH_3 collection air chamber for (A) 1Flat-MFCs, an extra gas chamber was set next to the MFCs. (B) CSA-MFCs, the MFCs were placed inside of an airtight chamber.

2.3. Topography and electrochemical analysis of Cu-blended 3D cathode.

To analyze the topography and structure of Cu-blended cathode, multiple characterization methods, including atomic force microscope (AFM), optical microscope, X-ray photoelectron spectroscopy (XPS), X-ray diffraction (XRD), Transmission electron microscopy (TEM), scanning electron microscope (SEM) and energy dispersive X-ray (EDX) were performed. To characterize the electrochemical performance of the Cu-blended 3D cathode, the linear sweep voltammetry (LSV), electrochemical impedance spectroscopy (EIS) and cyclic voltammetry (CV), chronoamperometry and Tafel analysis were conducted

using an electrochemical workstation (CH Instruments, Model 680, CHI760D). Referring to previous studies [29, 30], these tests were conducted with a three electrodes assembly and 0.2 M NaCl electrolyte. The details of methods can be seen at supporting information (section S1).

2.4. Measurement and analysis.

The voltage data were monitored by using a digital handheld multimeter (USB 6000, National Instruments, USA) and the external resistance was 1000 Ω for 1Flat MFCs and 100 Ω for CSA-MFCs except as noted. Current, power and other parameters were calculated by using basic electrical calculations. After more than 15 operation cycles , the MFCs power density curves were tested as previous described [31]. Water samples were collected with different time intervals (total volume of samples collected < 10% of electrolyte) for test. The concentrations of NO_2^--N, NO_3^--N and NH_4^+-N were tested by using the Konelab analyzer (20XT clinical analyzer, Thermo Fisher Scientific) while TN was determined by using TOC analyzer (TOC-L, Shimadzu). COD concentration was measured by using a colorimeter and COD regents (VWR).

To analyze NH_3 emission, NH_3 concentrations and percentages were calculated by equations 1-2:

$$C_{emNH3} = \frac{C_{asNH3}V_{as} - R_{air}t}{V_{anode}} \quad (1)$$

$$P_{emNH3} = \frac{C_{asNH3}V_{as} - R_{air}t}{V_{anode}\Delta C_{NH4-anode}} \times 100\% \quad (2)$$

Where C_{emNH3} is the emitted NH_3 concentration as N (mg/L); C_{asNH3} is NH_3 concentration as N (mg/L) at absorption solution; V_{as} is the volume of absorption solution (mL); R_{air} is the NH_3 increase rate due to air background, ug/h; t is the collection duration, h; V_{anode} is the net wastewater volume at MFC anode chamber, mL; P_{emNH3} is the emitted NH_3 percentage accounting for ammonium removal at wastewater, %; $\Delta C_{NH4-anode}$ is the change of ammonium concentration as N at MFC anode, mg/L.

3. Results and discussion

3.1. Ammonia emission from the typical MFCs with flat cathode

In this study, the NH_3 emitted from MFCs was collected directly (Fig. 3). It was found that the cathode biofilm played a key role for TN and NH_4^+-N removal and NH_3 emission (Fig. 3A and B). After 11 hours of operation, the 1Flat-MFCs feeding with dairy WW removed 82% of NH_4^+-N with cathode biofilm, and only 56% of NH_4^+-N without cathode biofilm. The cathode biofilm also benefits the reduction of NH_3 emission. With the cathode biofilm, the NH_3 emission was 0.82 mg-N/L, which accounted for 1.4% of NH_4^+-N removal in MFC. Without the cathode biofilm, the NH_3 emission increased by 15.5 times and reached up to 13.5 mg-N/L, which contributed to 25% of the total NH_4^+-N removal. The cathode biofilm could act as ammonium sinks as it consumed and oxidized ammonium. It probably also acts as a physical barrier to prevent the NH_3 emission, as previous studies found that the cathode biofilm was an effective barrier for ion and gas, such as OH^- and O_2 [32, 33].

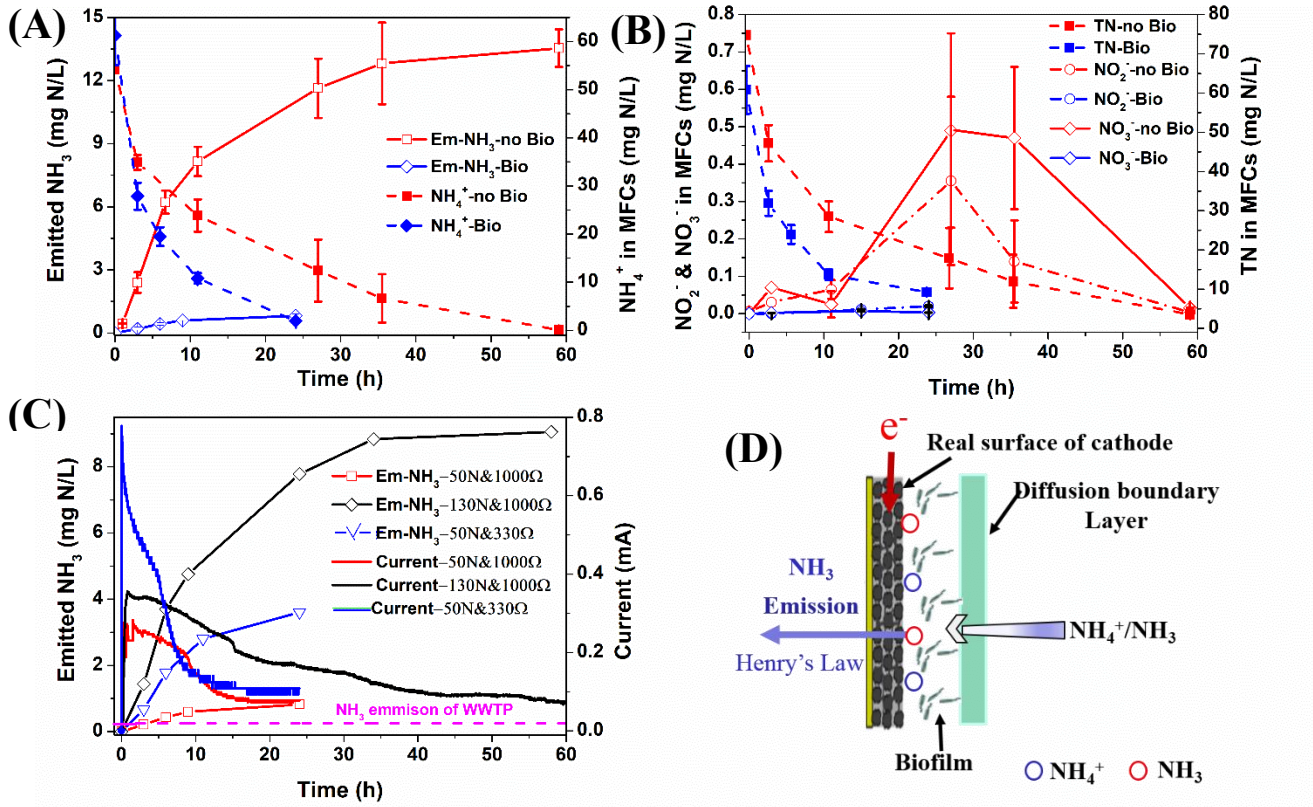

Fig. 3. Characters of N-pollutants removal and NH_3 emission under different conditions in 1Flat-MFCs: (A) NH_3 emission and NH_4^+ removal in the MFCs with and without cathode biofilm, respectively (The currents of MFCs were 0.25 mA; *no bio*: no cathode biofilm; *bio*: cathode biofilm; *Em*: emission). (B) TN, NO_2^- and NO_3^- removal in the MFCs with and without cathode biofilm, respectively; (C) Impact of current and influent ammonium concentration on NH_3 emission (*50N:* Influent *NH_4^+-N* concentration of 50 mg-N/L; *130N:* Influent *NH_4^+-N* concentration of 130 mg-N/L; *1000*Ω: external resistance of 1000 Ω; *330*Ω: external resistance of 330 Ω); (D) Potential emission process of NH_3/NH_4^+ in the surface of air cathode.

It was predicted that the high current could accelerate the emission of NH_3 [12]. This study had similar findings in 1Flat-MFCs (Fig. 3C). When the current reduced from around 0.6 mA to 0.25 mA, the NH_3 emission decreased from 3.60 mg-N/L to 0.82 mg-N/L. The initial NH_4^+-N concentration in the influent also had a significant influence on NH_3 emission (Fig. 3C). Increasing the feeding NH_4^+-N concentrations from around 50 mg-N/L to 130 mg-N/L led to the increase of NH_3 emission by 10 times.

Similar to NH_3 evaporation in wastewater or animal slurry [34, 35], the emission of NH_3 in MFC is affected by the FA concentration on the surface of the cathode (Fig. 3D). The FA concentration is determined by the total ammonia, pH and temperature [34]. The previous study found that the high current could generate much higher pH at identical MFCs and decreasing the external resistance from 1000 Ω to 100 Ω could increase pH from around 8 to 11 [32]. With this change in pH, the FA percentage in the total ammonia could increase from 5.6% to 98.3 % (assuming temperature is 25 °C).

Compared with the NH_3 emission in typical activated sludge (AS) WWTP (0.24 mg-N/L NH_3) [2], the emission from 1Flat-MFCs were 3.4-15 times of that when wastewater with a similar concentration of NH_4^+-N was treated (Fig. 3C). Given the high NH_3 emission, control and mitigation NH_3 emission is critical when MFC is used for wastewater treatment.

3.2. Ammonium removal mechanisms in MFCs

To benefit the control of NH_3 emission, the pathway of ammonium removal in MFCs was investigated by using nitrite-oxidizing bacteria (NOB) selective inhibitor. In this study, the MFCs with cathode biofilm removed more than 90% of the TN and the NH_3 emission only

accounted to less than 2% of this removal (Fig. 3). The majority of the removed TN could be converted to nitrogen gas through 3 typical pathways [36]: (1) Complete nitrification/denitrification; (2) Partial nitrification/denitrification; and (3) Anaerobic ammonia oxidation. The anaerobic ammonia oxidation is unlikely in MFCs as the microbial community analysis showed that anaerobic ammonia oxidizing bacteria (ANAMMOX) were not detected in MFC [9, 12, 13]. Both nitrification and denitrification bacteria were found in the anode and cathode biofilms [9, 12, 13]. When the selective inhibitor for NOB was added to MFC, it was found that the ammonium nitrogen removal was not affected (Fig. 4). Previous study pointed out that with the adding of selective inhibitor, the nitrite concentration would significantly increase (up to 80% of total nitrogen) in a complete nitrification/denitrification process dominated reactor [37]. However, the almost identical ammonium removal trends (with and without inhibitor) and the very low level of nitrite accumulation in the MFCs suggested that the complete nitrification/denitrification process did not contribute to the ammonium removal significantly in this MFCs. Therefore, the partial nitrification/denitrification process could be the main ammonium nitrogen removal pathway in MFCs. Previous studies showed that strict conditions, such as proper levels of DO, C/N ratio and pH, were needed to achieve simultaneously partial nitrification/denitrification (SND) in traditional wastewater treatment processes [36, 38]. This study indicated that MFCs could be ideal reactors for SND process.

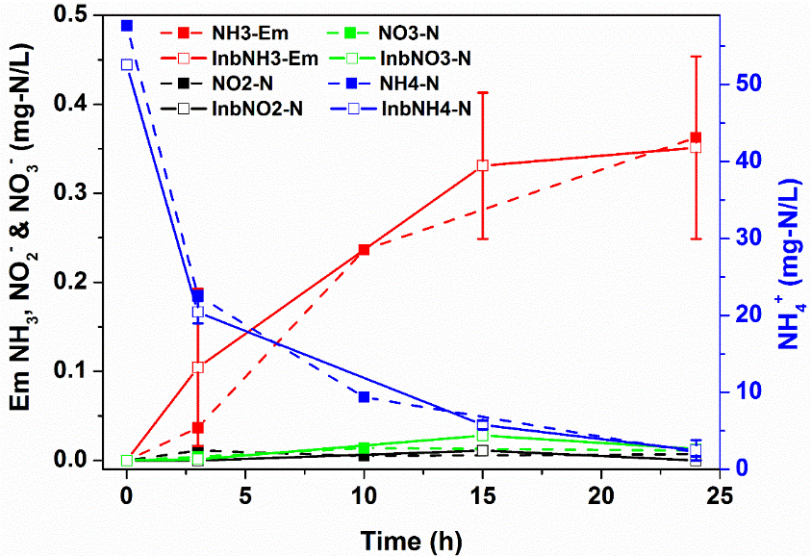

Fig. 4. N-pollutants removal and NH_3 diffusion process with and without NOB selective inhibitor (1Flat-MFCs, feeding with sodium acetate).

3.3. Cu-blended 3D cathode

3.3.1 Surface morphology and structure of Cu-blended 3D cathode

The Cu-blended 3D cathodes' physical characterizations were investigated to deepen the understanding of this novel cathode. The optical image obtained by microscope showed that Cu particles were well mixed with AC and PVDF and formed a uniform surface (Fig. 5A). TEM image revealed that the main catalyst (AC particles) homogeneously dispersed inside of PVDF (Fig. 5B). The air cathode acts as electron transfer carrier (attributing to AC) and provides oxygen diffusion pathway (PVDF) [25]. The homogeneous mixture of AC and PVDF can create large ORR area while decrease the proton/oxygen transfer distance, which benefits the electrochemical activity [39]. XRD analysis showed that the Cu-blended cathode (Fig. 5C) had diffraction peaks corresponding to the (111), (200), (220) of Cu (70-3039) and

(004) and (106) planes of C (26-1080). These results confirmed that all the compositions were well mixed and successfully projected on the surface of cathode.

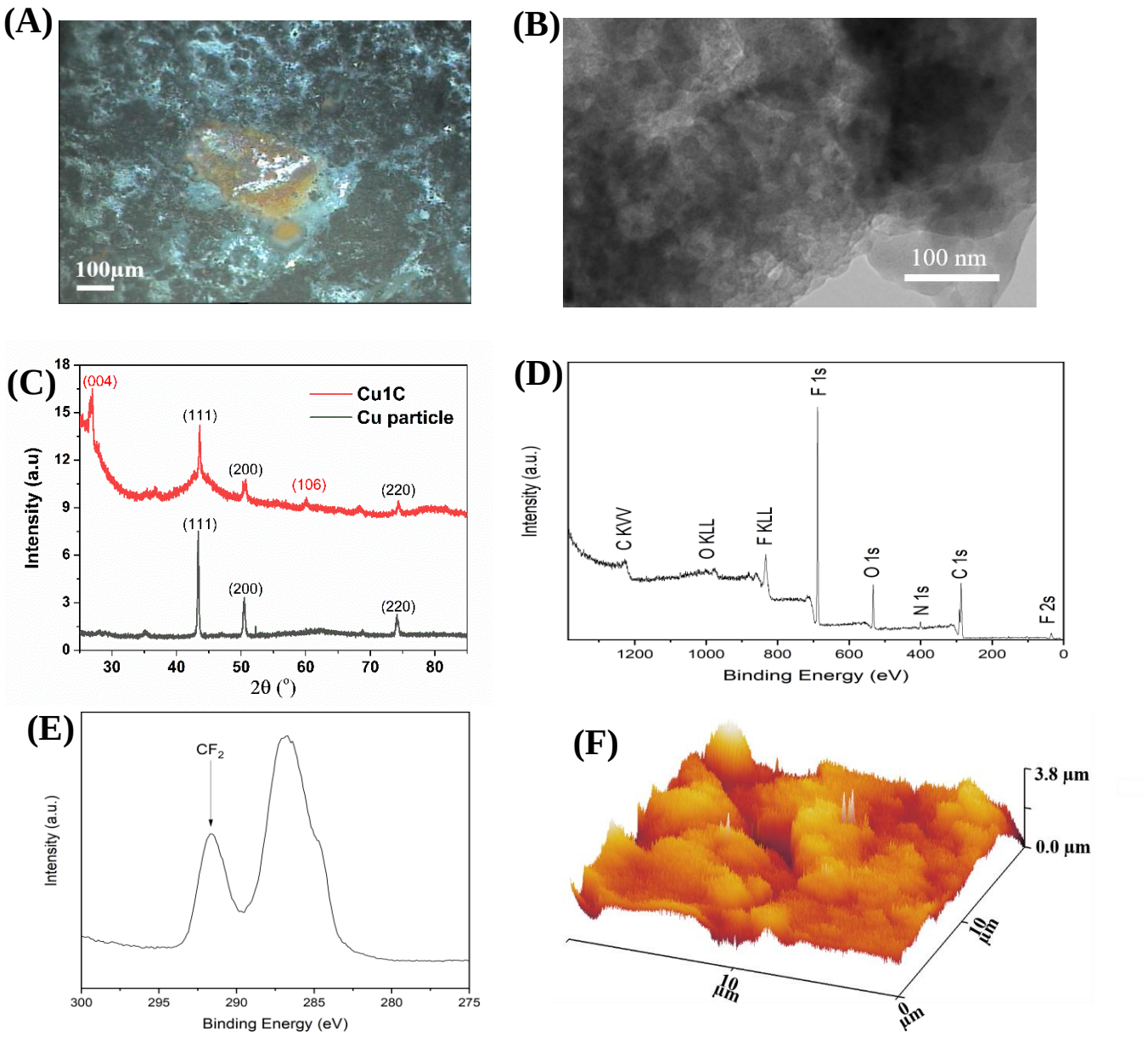

Fig. 5. (A) Optical image of Cu-blended cathode obtained by microscope with 10× objective. (B) The TEM image of Cu-blended cathode. (C) The XRD spectrum of Cu-blended cathode. (D) XPS survey spectra-full spectrum. (E) XPS survey spectra-zoomed figure of C1s area. (F)The 3D topography of Cu-blended cathode, obtained by AFM.

High-resolution XPS was performed to identify the elemental composition on the surface of Cu-blended cathode (Fig. 5D and E). The surface exhibits a complex C 1s lineshape. The most noteworthy feature of the C 1s region is the presence of a large peak at a binding energy of approximately 292 eV, which is typically ascribed to CF_2 arising from the PVDF. In a pure sample of PVDF, the feature at lower binding energies (~286 eV) has been found to have the same area as the CF_2 feature [40]. As activated carbon alone has multi-components and ill-defined lineshape [41], fitting of the C 1s region here was not performed. In comparison, the Cu particle/element was detected by both optical microscope and XRD while no Cu was seen by XPS even though the test was focusing on Cu particle area. This is likely attributed to the extreme surface sensitivity of XPS (test depth around 5 nm) and the Cu particle was likely covered by a thin layer (thicker than 5 nm) of AC and PVDF. Previous studies found that the Cu^{2+} had adverse effect on anode biofilm [42] while naked metal Cu in cathodes could release up to 0.05 mg/L of Cu^{2+} [13]. During the MFC operation, the thin layer covered on the surface of Cu particles in the Cu-blended cathode can reduce the formation and release of Cu^{2+}, which benefits the anode biofilm growth. In addition to chemical composition, the surface topography and roughness (R_q-RMS) of the Cu-blended cathode was also investigated by AFM (Fig. 5B). It was found that the surface was full of ridges and valleys. The cathode surface roughness was 500 ± 103 nm, which is much higher than that of carbon cloth based electrode (around 173 ± 8 nm) [33, 43]. This high roughness can significantly increase the surface area of cathode, resulting in a low charge transfer resistance (confirmed by EIS test), which benefits the power generation [43]. In addition, the coarse and large surface area can supply extra space for cathode biofilm growth, which is critical for both NH_3 emission control and power performance improvement [33].

3.3.2 Electrochemical characterization of Cu-blended 3D cathode

Multiple electrochemical tests were performed to investigate the electrochemical activity of Cu-blended cathode. LSV of different number of novel cathodes were conducted with the voltage range of -0.1V to 1 V. The results showed that all LSV curves exhibited similar trend, regardless of cathode number (Fig 6A). It was observed that an increase in the active surface area by 300% (from 28.3 cm^2 to 113.2 cm^2) produced an enhancement of 33% on the current density. This suggests that the larger the surface area, the more efficient is the catalyst. These results indicate that the electrochemical behavior can be improved when enlarging cathodes for practical MFCs application. In comparison to previous studies of electrodes [44], the current density achieved in this work was significantly higher. For instance, at 1.0 V versus Ag/AgCl, the Cu-blended cathode achieved current density of around 15 A/m^2, which was higher than that of MgO (around 5 A/m^2) and Pt/C electrodes (around 8-10 A/m^2) [44]. Chronoamperometry studies were conducted to investigate the stability of Cu-blended cathode (Fig. S3). During the test, the cathode was subjected to +0.3 V for a period of 36 h. Initially, the current-time response showed a notorious current density decrease corresponding to the activation of the catalyst. This activation process lasted for 15 min. After 15 min, the catalytic performance improved, resulting in a consistent increase in current density. After 14 h, the current density reached a peak value of 6.5 A/m^2, twice of its initial current density (3.3 A/m^2). Then the current density slowly decreased to 2.1 A/m^2 after 36 h, which was still 64% of the initial value. These results demonstrated the good current density performance of Cu-blended cathode over time. In addition, Tafel analysis was conducted to determine the kinetic parameter of Cu-blended cathode. With the intercept of -4.2 in Tafel plot (Fig. S4), the corresponding exchange current density was 0.63×10^{-4} A/cm^2. In contract

to a previous study using carbon-based cathode [45], the novel cathode developed in this study exhibits higher exchange current density which confirms the advantage of Cu-blended electrode.

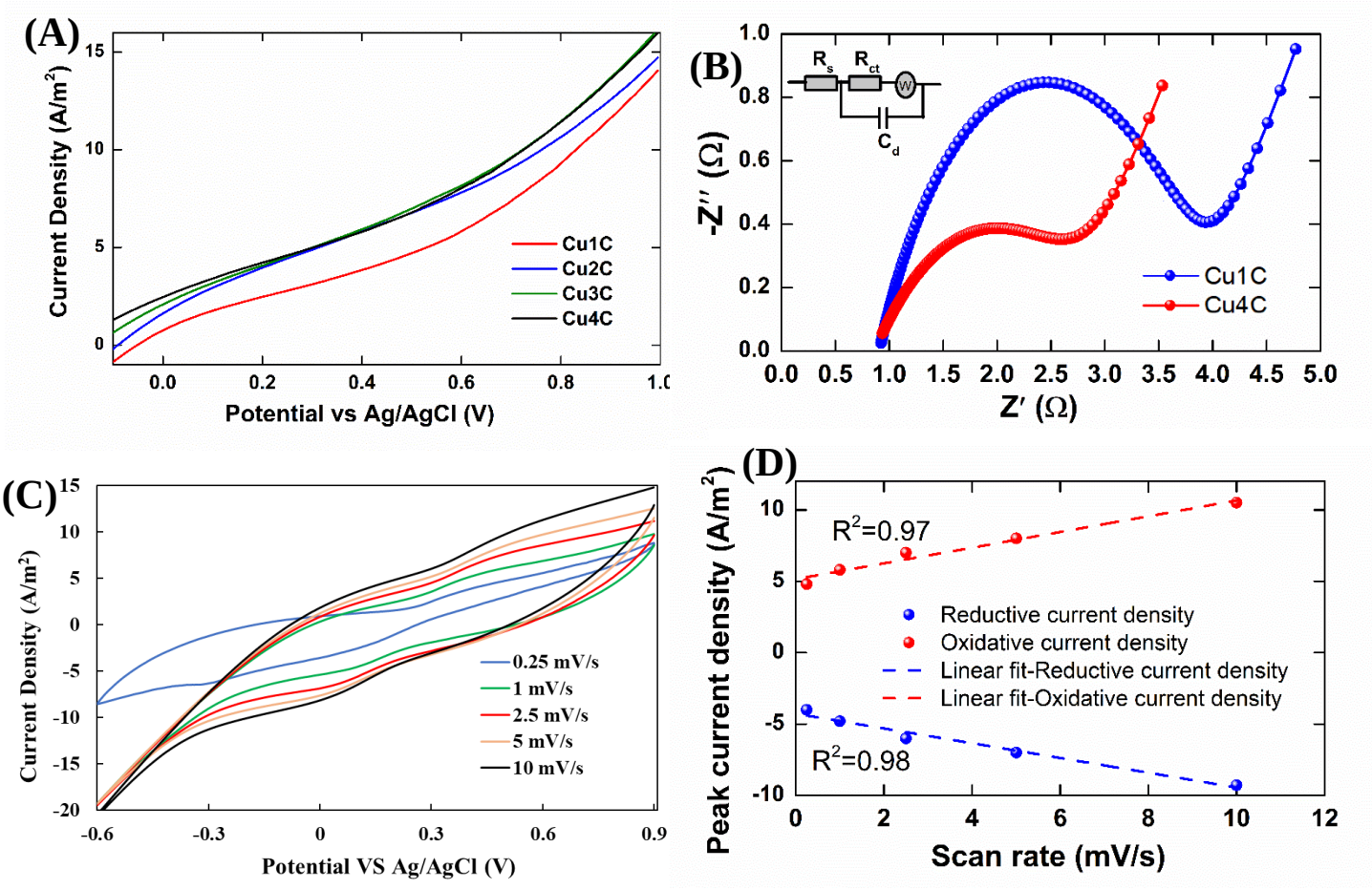

Fig. 6. (A) LSV curves for Cu-blended cathode with different numbers (Cu1C: 1 Cu-blended cathode. All made as the earlier description in Section 2.1). (B) Nyquist plots of Cu1C and Cu4C. The ac impedance spectra are fitted with an equivalent circuit-the inserted figure. (C) CV plots at the scan rate from 0.25 to 10 mV/s (Cu1C used at test). (D) Linear relationship between redox peaks current density and scan rate of Cu-blended cathode (Cu1C used at test).

Electrochemical impedance spectroscopy (EIS) was conducted at the frequency range of 100 kHz to 5 mHz to investigate the physical properties of Cu-blended cathode. The Nyquist plots and the equivalent circuit used are shown in Fig. 6B while the fitting parameters are summarized in Table S1. For a single Cu-blended cathode, the Ohmic resistance (Rs) and charge transfer resistance (Rct) was 4.3 Ω and 3.0 Ω, respectively, which were remarkably lower than the carbon cloth (266.6 Ω) and Pt-carbon cloth (11.5 Ω) electrodes reported in previous studies [39, 43]. This is likely due to the large surface area of the Cu-blended cathode. With the novel 3D design, the proposed cathode has a surface area of 28.3 cm^2, which is larger than previous proposed electrodes (such as 7 cm^2 in [43]). In addition, AFM results indicated that the surface roughness of Cu-blended electrode mixing with AC, Cu particles and PVDF was approximately 2 times higher than that for carbon cloth electrode. The EIS of 4 Cu-blended cathodes was also conducted and it was found that both Rs and Rct further reduced to 0.9 Ω and 2.1 Ω, respectively. These results indicate that a number of electrodes used together can enhance MFCs electrochemical properties.

In order to further explore the electrochemical properties of Cu-blended electrodes, CV analysis was conducted. It was initially measured in 0.2 M NaCl solution with the scan rate of 5 mV/s. However, there were no redox peaks, while both large capacitance and a significant resistance contribution were observed (Fig. S5). The latter may be due to the extra contact resistance produced when the film was deposited onto the carbon-base structure. Therefore, in order to further analyze the electrochemical proprieties of these cathode electrodes, CV tests with different scan rates (0.25 - 15 mV/s) were performed on electrolyte of 5 mM $K_3[Fe(CN)_6]$ + 5mM $K_4[Fe(CN)_6]$ + 0.1 M KCl (Fig. 6C and D). It was found the

proposed cathode exhibited one broad redox couple at around 0.5 V and 0 V (vs Ag/AgCl), corresponding to the anodic and cathodic reactions respectively. The redox couple may be attributed to the oxidation and reduction of iron species on the electrode surface. The board shape of both redox peaks suggests that the oxidation or the reduction of iron species takes place gradually. This is normally attributed to different activation sites on the surface. Figs 6C and D showed that (i) the peak current of both redox peaks are proportional to the scan rate, and (ii) the redox peak potentials, remained constant at 0.5 V and 0 V respectively. The former suggests that the reaction is not limited by diffusion. The latter is commonly found in surface reactions with rapid electron transfer kinetics. In general, the redox peaks of this test are not clearly defined due to the large contribution of the double layer capacitance. For instance, increasing the scan rate to 15 mV/s (Fig. S6), the redox peaks are barely defined, which suggesting that the double layer capacitance becomes the main contribution to the current exchange.

3.3.3 Ammonia emission from the 3D cathode and Cu-blended 3D cathode

The MFCs with 3D cathode (CSA) was assambled to control NH_3 emission (Fig. 1 and Table 1). With the 3D cathode, the MFCs power performance was improved while the NH_3 emission was significantly reduced (Fig. 7A). Feeding with the diary wastewater, the NH_3 emission reduced from 3.60 mg-N/L in 1Flat to 2.90 mg-N/L in CSA1C, while the current of CSA1C (around 1.1 mA) was much higher than that of 1Flat (around 0.6 mA). Increasing the number of cathodes could further reduce the NH_3 emission and improve the power performance. The NH_3 emission from CSA2C was further reduced to 2.13 mg-N/L and the current increased to around 1.5 mA. However, these NH_3 emission values were still much

higher than that of typical WWTP (0.24 mg-N/L NH_3) and more effective method is needed to reduce the NH_3 emission further.

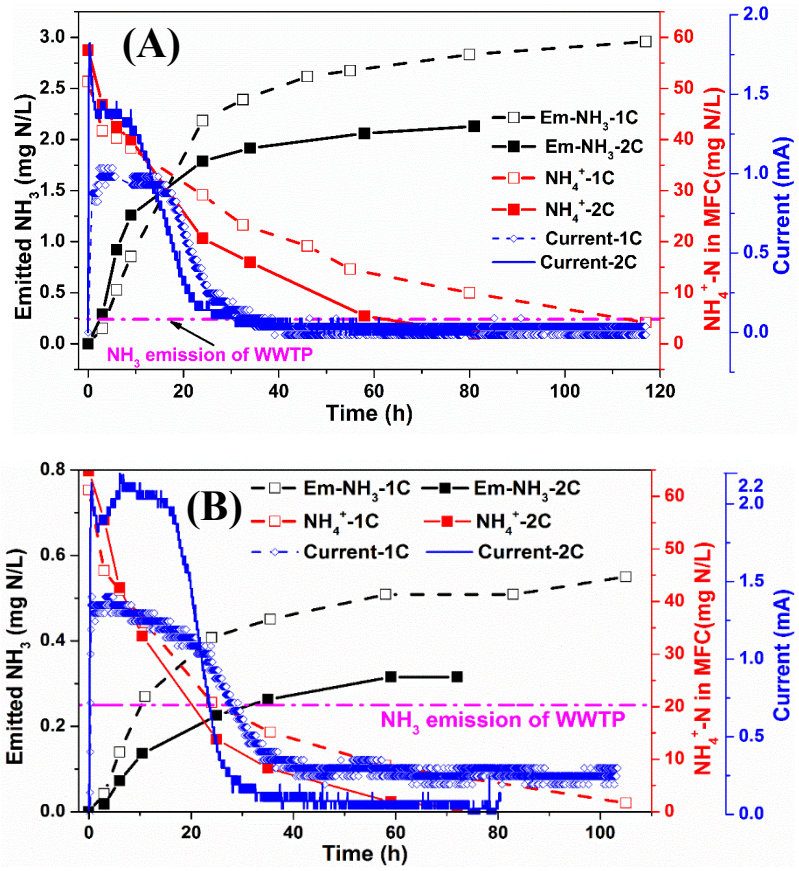

Fig. 7. NH_3 emission change with the cathode modification: (A) NH_3 emission of CSA-MFCs with different cathode numbers (*CSA1C*: 1 cathode; *CSA2C*: 2 cathodes; *Em*: emission). (B) NH_3 emission of CSA Cu-MFCs with different cathode numbers (the cathode was blended with Cu particles; *CSACu1C*: 1 cathode; *CSACu2C*: 2 cathodes; *Em*: emission).

Previous study found that copper (Cu) could increase the amount of denitrification bacteria while inhibit the growth of NOB [13], which could benefit the mitigation of NH_3 emission. To control the NH_3 emission, in this study Cu-blended 3D cathodes were

developed. After 2-month operation, the Cu-blended 3D cathodes emitted much lower NH_3 than the normal 3D cathode, at the same time the current generation increased from around 1.0-1.5 to 1.5-2.0 mA (Fig. 7B). The emission of CSACu1C and CSACu2C were only 19.0% (0.55 mg-N/L) of CSA1C and 13.9% (0.32 mg-N/L) of CSA2C, respectively. The NH_3 emission of 0.32 mg-N/L in CSACu2C was only accounted for 0.49% of the total NH_4^+-N removal in MFCs. In a typical activated sludge WWTP, NH_3 emission contributed to 1.08% of the total NH_4^+-N removal[2]. These results indicated that the MFCs with Cu-blended 3D cathodes have great potential to prevent NH_3 emission and improve power generation performance.

It was also noticeable that the NH_3 emission of CSACu2C in the first 6 h (0.07 mg-N/L) was much lower than that of CSACu1C (0.14 mg-N/L), although the current of CSACu2C (2 mA) was higher than that of CSACu1C (1.3 mA) (Fig. 7B). According to previous theoretical study[46], the cathode surface pH was determined by the current density rather than the total current (equation 3-5).

$$\eta_{act} = (\ln i - \ln i_0) \bullet \frac{RT}{anF} (3)$$

$$\eta_{[OH^-]} = \eta_{total} - \eta_{act} (4)$$

$$\eta_{[OH^-]} = \frac{RT}{nF} \ln \frac{C^a_{OH^-}}{C^0_{OH^-}} (5)$$

η_{act} is the activation loss; $\eta_{[OH^-]}$ is the potential loss caused by OH^- concentration; η_{total} is the total potential loss, obtained from experiment; i is the electrical current density; $C^a_{OH^-}$

is the actual concentration of OH^-; other parameters such as i_0 (exchange current density), a (Constant), $C^0_{OH^-}$ (reference concentration of OH^-),R (universal gas constant), T (temperature), F (Faraday constant) could be assumed as constants with similar experiment conditions.

Combined equations 3-5, the cathode surface pH ($-\lg(C^a_{OH^-})$) could be calculated by the current density (i). The cathode surface pH, which affects the FA significantly, was very sensitive to the current density at the range 0-1A/m^2 [46]. It could increase from 7.5 to 11 when the current density increased from 0 A/m^2 to 1 A/m^2. In this study, though the total current in CSACu2C was higher than CSACu1C, its current density was lower. Therefore, its NH_3 emission was less.

Table 2
Summary of NH_3 emission studies

	Wastewater	Configuration	Initial NH_4^+-N	Current	Current density	Cathode biofilm?	Emitted NH_3/removal NH_4^+-N	Ref
			mg/L	mA	A/m^2		%	
A	Dairy WW	Cu modified CSA	54.2	2	0.50	Yes	0.07%	This study
B	Dairy WW	Flat	126.9	0.3	0.43	No	36.1%	This study
C	Swine manure	Flat	188	0.18	0.26	NA	Dominated by NH_3 emission	[12]
D	Domestic WW	Flat	<30	9	0.30	Yes	Dominated by biological removal	[9]
E	Human urine	Flat	around 4000	1.1-5	0.11-0.5	No	NA	[19]

WW: wastewater; NA: not available

Table 2 summaries some of the NH_3 emission studies. Both physic-chemical NH_3 emission and biological removal were claimed as the dominant pathway for ammonium removal (Table 2). In this study, it was evident that the major ammonium removal could be due to either physical–chemical process, or biological process, or both, which depended on the operation condition of MFCs. With the changes of conditions (influent concentration, current density, cathode structure, blended particles and cathode biofilm), NH_3 emission

could be effectively enhanced (recovering NH_3 from high ammonium WW, such as animal's manure and human urine) or mitigated (low ammonium WW, such as domestic WW).

3.3.4 Cu-blended cathode power performance

The CSACu4C (4 Cu-blended cylindrical cathodes, Section 2.1) was used to investigate the power generation performance of MFCs employed with the novel Cu-blended 3D cathode. To make the results comparable to previous studies [26-28], raw dairy WW added by PBS was used in this experiment. After 1 month of operation, the highest value of maximum power density obtained was 14.4 W/m^3, which was comparable to the highest values reported in previous studies (Table 3). The results obtained by CSACu4C clearly showed that the CSA structure employing with Cu-blended cathode could not only control NH_3 emission but also effectively harvest the electricity. Given the significant influence of cathode area on MFCs' performance and the convenient cathodes increase of CSA structure, it is reasonable to conclude that the better performance could also be achieved by CSA structure when more cathodes are employed.

Table 3. Summary of power performance obtained from different MFCs fed with dairy wastewater

NO.	MFC configuration	Net volume	Power density	CE	reference
		(mL)	(W/m^3)	(%)	
1	SC-CSACu4C [a]	250	14.4	16.6 ± 5.5	This study
2	SC-MFC	45	0.442	3	[47]
3	SC-Tubular MFC	90	20.2	27	[26]
4	DC-MFC	700	1.157	NA	[48]
5	DC-MFC	480	1.1	14.2	[49]
6	DC-MFC	300	2.7	17	[14]
7	DC-MFC	350	5.1	24	[28]
8	DC-MFC	855	13.1	<20	[27]

[a] results obtained at test condition of with raw dairy WW adjusting by PBS and temperature of 30 °C, which is consistence with previous reports [26, 27]. SC=single chamber, DC=double chamber, NA=Not available.

3.3.5 Long-term performance of Cu-blended cathode

Two identical MFCs of CSACu4C feeding with diluted dairy WW were operated for 14 months to investigate the long-term performance of the Cu-blended cathode (Fig. 8). Regarding the power generation, the maximum power density increased from 3.6 W/m^3 after 1 week of operation to 4.3 W/m^3 after 2 weeks of operation and reached the highest maximum power density of 5.5 W/m^3 after 2 months of operation (Fig. 8A). This power performance could sustain around 6 months. However, with the operation duration increasing to 14 months, the maximum power density significantly decreased to 1.3 W/m^3, only 23.6% of the optimum power density. This is most likely due to the cathode fouling, which was commonly reported at long-term practical application of MFCs [16, 27, 50].

In contrast, the NH_3 emission showed a significantly different tendency (Fig. 8B). The NH_3 emission of MFCs decreased from 1.1 mg-N/L in week 1 to 0.37 mg-N/L in 2 week. With the operation increasing to 2 months, the emission level the NH_3 emission reduced to

0.037 mg-N/L, which was only accounted for 0.068% of the total NH_4^+-N removal in MFCs, and was about 6.3% of the NH_3 emission from the typical WWTPs. It was very noticeable that no NH_3 emission was detected when the operation time increasing to 14 months. Fig. 8C and D showed the NH_4^+ removal capacity of CSACu4C within long-term operation. It is noticeable that the ammonium removal rates showed excellent agreement with an assumption of first-order kinetics (average value of R^2 =0.90, Fig. 8D and Table S1), regardless of operation durations. However, the removal rates varied significantly. In week 1, the removal rate was very low (-0.005 h^{-1}), it then quickly increased to -0.017 h^{-1} in week 2. Expanding the operation duration to 2 months, the removal rate reached the highest value of -0.089 h^{-1}. Different from the plummeting of power generation, the ammonium removal capacity kept relatively stable (-0.049 h^{-1}) after 14 months of operation. Fig. 8E showed that more than 83% of the TN was removed after month 2, suggesting that NH_3 emission contributed little to the TN removal.

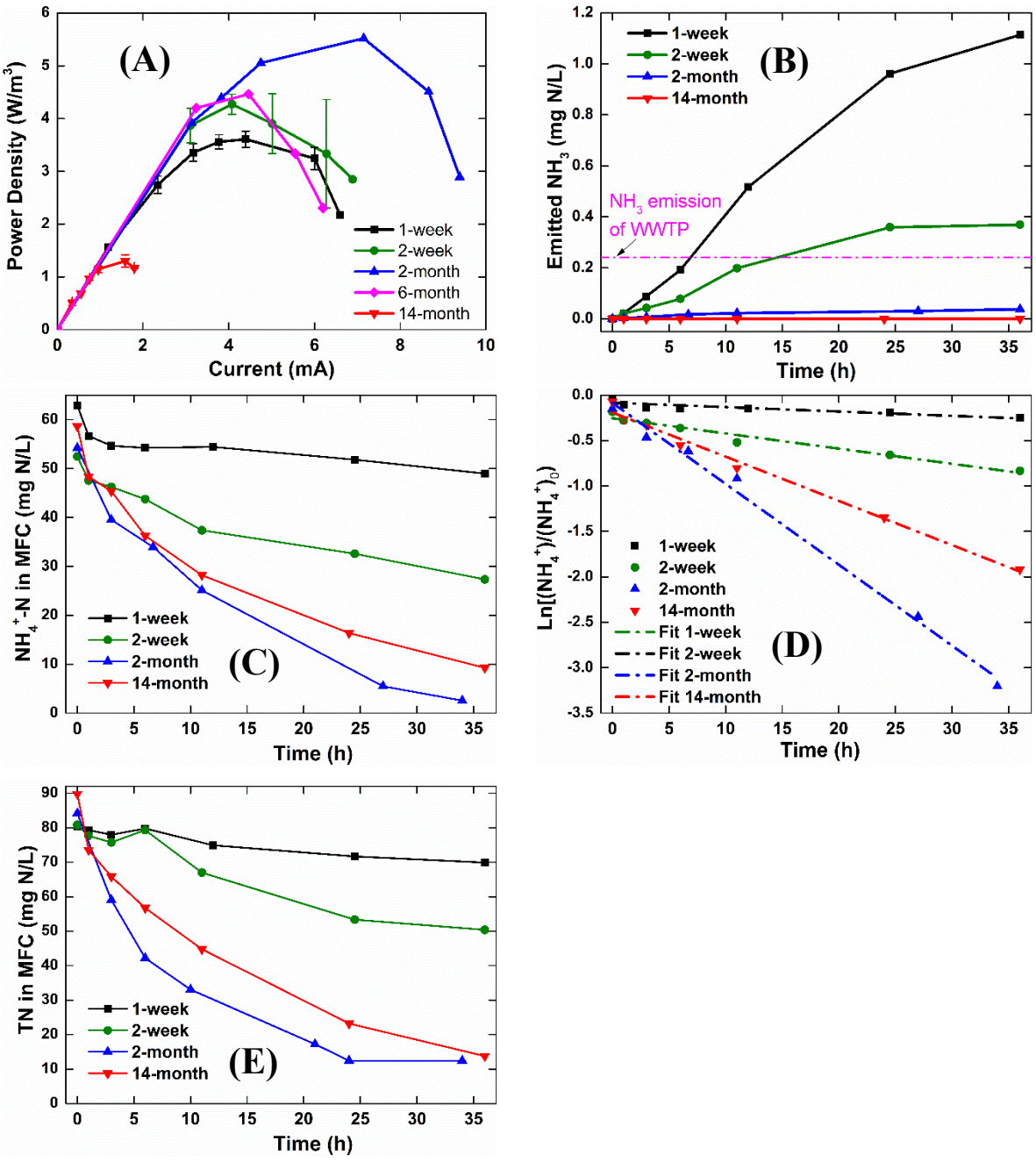

Fig. 8. (A) Power density curves of CSACu4C in long term of operation. (B) NH_3 emission of CSACu4C in 14 months of operation. (C) NH_4^+ removal in CSACu4C with 36 h in 14 months of operation. (D) First-order reaction fitting for NH_4^+ removal. (E) TN removal in CSACu4C with 36 h in long term of operation.

The surface of Cu-blended 3D cathode before and after operation was investigated by SEM-EDX mapping the elements distribution on cathodes (Fig. 9). As the mixture used in Cu-blended 3D cathode contained AC, PVDF (formula of -$(C_2H_2F_2)_n$- and Cu, high content of C, Cu and F elements were found in both new and old cathodes. O and S elements presented in the new cathode but significant increased in the old cathode. It is noticeable that significant accumulation of Ca was found in the old Cu-blended 3D cathode, which was absent in the new cathode. Similarly, P and Fe also accumulated in the old cathode. Elements study pointed out that the dairy wastewater are rich of all the elements discussed above [51]. This is especially true for the element of Ca which is one of the richest elements in dairy products with up to 2 g/L-concentration [51]. These results clearly showed that salt precipitation played a significant role in cathode fouling. Similar findings were also reported by previous studies [52, 53]. Zooming in the cathode surface (Fig. S7), it was found that the new cathode surface was full of pores with different sizes (ranging from sub-micron to 40 μm). However, after 14 months of operation, these pores disappeared which was probably due to the salt precipitation. Low porosity of the cathode could reduce the diffusion of oxygen, resulting in poor power performance. Conversely, low porosity could benefit the mitigation of NH_3 emission, which contributed to the zero emission of NH_3 after 14-month of operation.

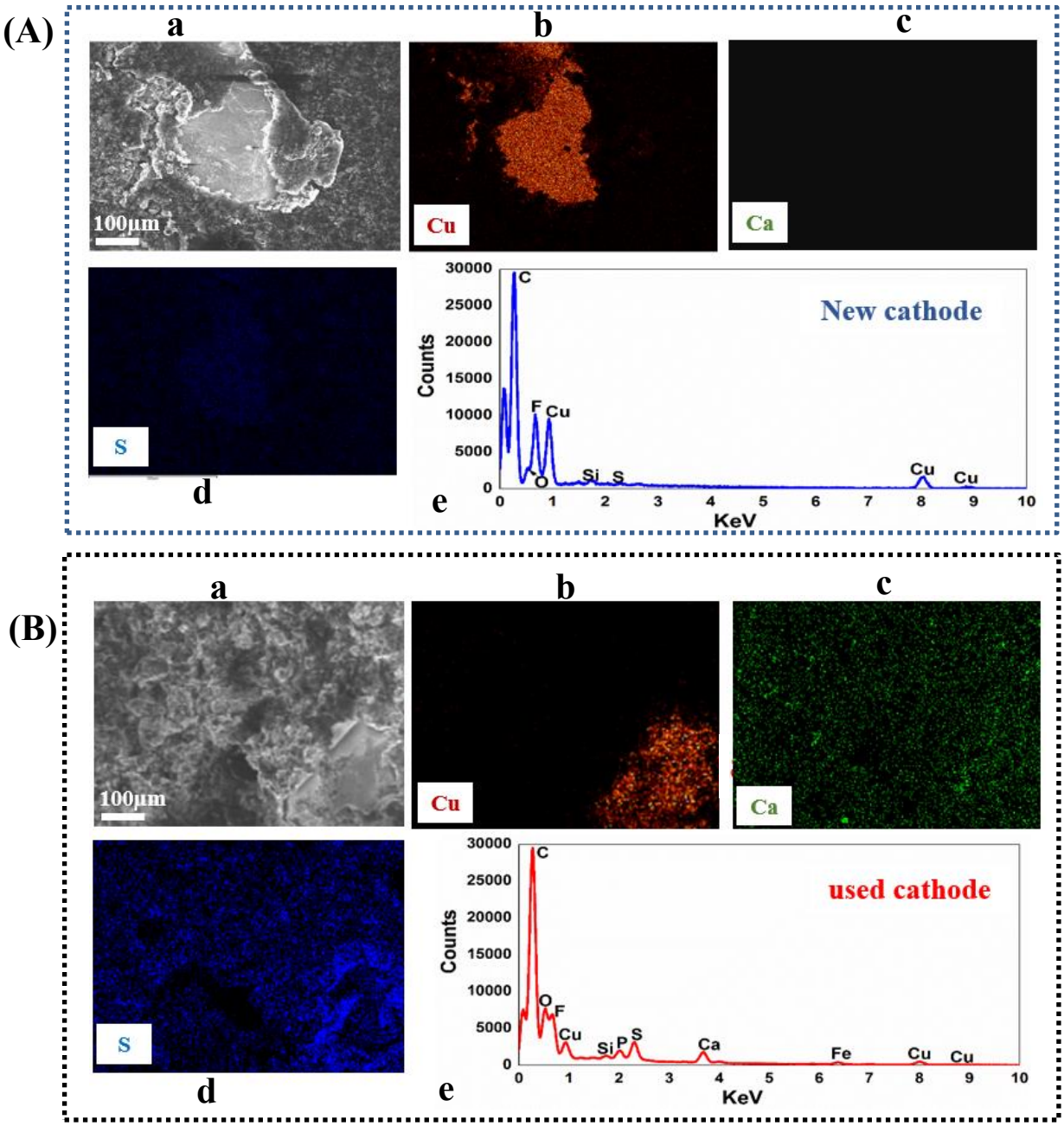

Fig. 9. (A) SEM images and elements mapping of Cu, Ca and S (a-d) and Full EDX spectra (e) of new Cu-blended cathode. (B) SEM images and elements mapping of Cu, Ca and S (a-d) and Full EDX spectra (e) of used Cu-blended cathode after 14 months of operation.

3.4 Implications for MFCs' design and operation

To reduce NH_3 emission, efforts are needed to either reduce the NH_3 production and/or block its transport pathway. The findings of this study suggest that the NH_3 emission from MFCs could be decreased by growing cathode biofilm, lowering the influent concentration of NH_4^+-N and decreasing the cathode current density. In practical application, new cathode without biofilm could lead to serious NH_3 emission and pre-grown biofilm could be a feasible method to mitigate this emission. Increasing external resistance is another method to lower cathode current density and NH_3 emission. However, this would hinder the harvesting of high current, which is critical for the practical use of relatively low current generated by MFCs. Structure modification could be the practical and convenient approach for controlling NH_3 emission. Both theoretical and experimental results showed that high current and low NH_3 emission could be simultaneously achieved by increasing CSSA, which could lower the current density. However, how to increase CSSA is one of the major bottlenecks limiting the practical application of MFC technology for wastewater treatment. Different from the most widely used graphite fiber brush anode (GFB anode) with sufficient surface area, it is difficult to increase the CSSA in the MFCs employing GFB anode [54], as the compact electrode configuration (such as sandwiched electrodes), which is commonly used to increase the CSSA, is not suitable to the GFB anode. Approaches such as placing the cathode on each side of the chamber (in cubic shape MFCs) or wrapping cathode around the GFB (in tube shape MFCs) were proposed to increase the cathode surface areas. However, these approaches cannot increase the CSSA efficiently in large MFCs, as the CSSA achieved by these approaches could decrease with the increase of the MFCs chamber volumes. The novel

structure of CSA employed with Cu-blended 3D cathode developed in this study could increase cathode surface area conveniently.

In the study of CSACu4C, it is noticeable that the NH_3 emission reduced to about 6.3% of the NH_3 emission from the typical WWTPs. Meanwhile, it also showed very competitive performance in terms of the pollutants removal (88.1%-COD and 92.8%-TN removal in 24 h, reaching discharge limiting value of EU, Fig. 10). Given the good performance achieved by CSA4Cu, the novel structure proposed here has great potential to further improve the power performance and pollutants removal (especially for NH_3 emission control) if the 3D cathode could be made small enough by novel technology such as 3D printer and employed as many as necessary.

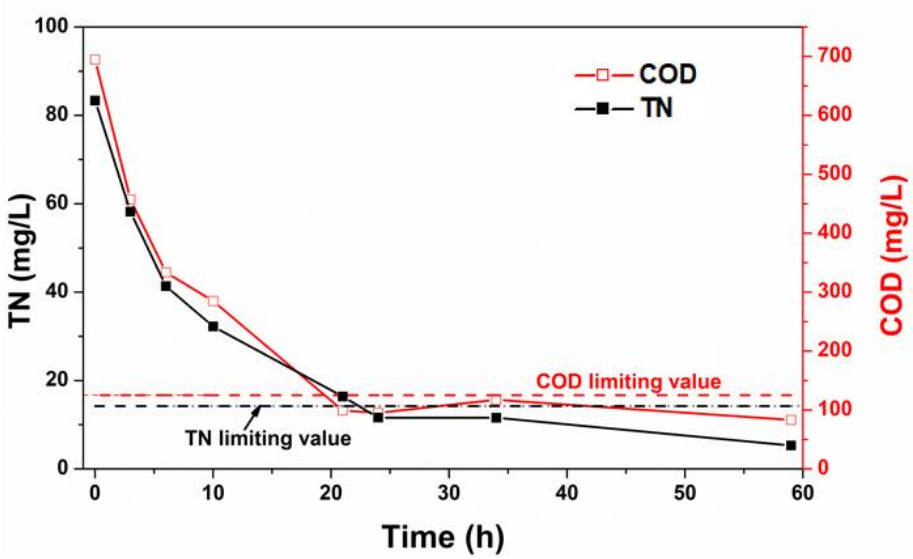

Fig. 10. TN and COD removal of CSACu4C in first 6 month.

In terms of the fouled cathode, it has been reported that the regeneration of cathode is not a cost-effective choice [55]. Given the high NH_4^+-N removal capacity and zero NH_3 emission

but low power generation, the fouled cathode could be used to enhance the removal of NH_4^+-N or treat the ammonium-rich WW with stringent NH_3 emission requirement, to maximize its benefit and lower the operational cost.

4. Conclusions

This paper studied the NH_3 emission process in MFCs and investigated possible control methods. The study found that the NH_3 emission reduced with the grown of cathode biofilm, the decrease of ammonium concentration in influent and the decrease of current density. It was also found that the major ammonium removal could be due to either physical–chemical process, or biological process, or both, which depended on the operation condition of MFCs. With the changes of conditions (influent concentration, current density, cathode structure, blended particles and cathode biofilm), NH_3 emission from MFCs could be effectively enhanced or mitigated. The Cu-blended 3D cathode was proposed to enhance power performance and control NH_3 emission. With the novel design, the surface roughness and geometry area were significantly increased, which resulting in low electrode charge transfer resistance of only 2.1 Ω. Employing with Cu-blended cathode, MFCs achieved good power performance and high pollutants removal (14.4 W/m^3, 88.1%-COD and 92.8%-TN removal). More importantly, the Cu-blended 3D cathode reduced the NH_3 emission to 0.037 mg-N/L, which was 6.3% of that in the WWTP. The work not only reveals the NH_3 emission mechanism but also supply a novel method to effectively control the emission as well as improve power performance.

Acknowledgements

We appreciate financial support from the China Scholarship Council (201506210089 and 201608300005), the Irish Department of Agriculture, Food and the Marine (13F507) and the School of Engineering Scholarship at Trinity College Dublin.

Appendix A. Supplementary data

Supplementary data associated with this article can be found in another file (7 Figures and 2 tables).

References

[1] J.W. Erisman, M.A. Sutton, J. Galloway, Z. Klimont, W. Winiwarter, How a century of ammonia synthesis changed the world, Nature Geoscience 1 (2008) 636.
[2] C. Zhang, X. Geng, H. Wang, L. Zhou, B. Wang, Emission factor for atmospheric ammonia from a typical municipal wastewater treatment plant in South China, Environmental pollution 220 (2017) 963-970.
[3] S.N. Behera, M. Sharma, Transformation of atmospheric ammonia and acid gases into components of PM 2.5: an environmental chamber study, Environmental science and pollution research 19 (2012) 1187-1197.
[4] J. Plautz, Ammonia, a poorly understood smog ingredient, could be key to limiting deadly pollution, Science doi:10.1126/science.aav3862 (2018).
[5] Y. Wu, B. Gu, J.W. Erisman, S. Reis, Y. Fang, X. Lu, X. Zhang, PM2. 5 pollution is substantially affected by ammonia emissions in China, Environmental pollution 218 (2016) 86-94.
[6] S.N. Behera, M. Sharma, V.P. Aneja, R. Balasubramanian, Ammonia in the atmosphere: a review on emission sources, atmospheric chemistry and deposition on terrestrial bodies, Environmental Science and Pollution Research 20 (2013) 8092-8131.
[7] S.M. Roe, M.D. Spivey, H.C. Lindquist, K.B. Thesing, R.P. Strait, Estimating ammonia emissions from anthropogenic nonagricultural sources-Draft final report, Emission Inventory Improvement Program, US Environmental Protection Agency (2004).
[8] B.E. Logan, K. Rabaey, Conversion of wastes into bioelectricity and chemicals by using microbial electrochemical technologies, Science 337 (2012) 686-690.
[9] Y. Park, S. Park, V.K. Nguyen, J. Yu, C.I. Torres, B.E. Rittmann, T. Lee, Complete nitrogen removal by simultaneous nitrification and denitrification in flat-panel air-cathode

microbial fuel cells treating domestic wastewater, Chemical Engineering Journal 316 (2017) 673-679.
[10] D. Wu, F. Sun, F.J.D. Chua, Y. Zhou, Enhanced power generation in microbial fuel cell by an agonist of electroactive biofilm–Sulfamethoxazole, Chemical Engineering Journal (2019) 123238.
[11] M. Li, S. Zhou, Y. Xu, Z. Liu, F. Ma, L. Zhi, X. Zhou, Simultaneous Cr (VI) reduction and bioelectricity generation in a dual chamber microbial fuel cell, Chemical Engineering Journal 334 (2018) 1621-1629.
[12] J.R. Kim, Y. Zuo, J.M. Regan, B.E. Logan, Analysis of ammonia loss mechanisms in microbial fuel cells treating animal wastewater, Biotechnology and bioengineering 99 (2008) 1120-1127.
[13] J. Myung, W. Yang, P.E. Saikaly, B.E. Logan, Copper current collectors reduce long-term fouling of air cathodes in microbial fuel cells, Environmental Science: Water Research & Technology 4 (2018) 513-519.
[14] E. Elakkiya, M. Matheswaran, Comparison of anodic metabolisms in bioelectricity production during treatment of dairy wastewater in Microbial Fuel Cell, Bioresource technology 136 (2013) 407-412.
[15] N. Yang, G. Zhan, D. Li, X. Wang, X. He, H. Liu, Complete nitrogen removal and electricity production in Thauera-dominated air-cathode single chambered microbial fuel cell, Chemical Engineering Journal (2018).
[16] X. Jin, F. Guo, W. Ma, Y. Liu, H. Liu, Heterotrophic anodic denitrification improves carbon removal and electricity recovery efficiency in microbial fuel cells, Chemical Engineering Journal 370 (2019) 527-535.
[17] X. Zhang, F. Zhu, L. Chen, Q. Zhao, G. Tao, Removal of ammonia nitrogen from wastewater using an aerobic cathode microbial fuel cell, Bioresource technology 146 (2013) 161-168.
[18] C.-P. Yu, Z. Liang, A. Das, Z. Hu, Nitrogen removal from wastewater using membrane aerated microbial fuel cell techniques, Water research 45 (2011) 1157-1164.
[19] P. Kuntke, K. Śmiech, H. Bruning, G. Zeeman, M. Saakes, T. Sleutels, H. Hamelers, C. Buisman, Ammonium recovery and energy production from urine by a microbial fuel cell, Water research 46 (2012) 2627-2636.
[20] P. Kuntke, M. Geleji, H. Bruning, G. Zeeman, H. Hamelers, C. Buisman, Effects of ammonium concentration and charge exchange on ammonium recovery from high strength wastewater using a microbial fuel cell, Bioresource technology 102 (2011) 4376-4382.
[21] W.A. Tarpeh, J.M. Barazesh, T.Y. Cath, K.L. Nelson, Electrochemical Stripping to Recover Nitrogen from Source-Separated Urine, Environmental science & technology 52 (2018) 1453-1460.
[22] P. Zamora, T. Georgieva, A. Ter Heijne, T.H. Sleutels, A.W. Jeremiasse, M. Saakes, C.J. Buisman, P. Kuntke, Ammonia recovery from urine in a scaled-up Microbial Electrolysis Cell, Journal of Power Sources 356 (2017) 491-499.
[23] S. Lu, H. Li, G. Tan, F. Wen, M.T. Flynn, X. Zhu, Resource recovery microbial fuel cells for urine-containing wastewater treatment without external energy consumption, Chemical Engineering Journal (2019).
[24] K. Song, M. Mohseni, F. Taghipour, Application of ultraviolet light-emitting diodes (UV-LEDs) for water disinfection: A review, Water research 94 (2016) 341-349.

[25] W. Yang, W. He, F. Zhang, M.A. Hickner, B.E. Logan, Single-Step Fabrication Using a Phase Inversion Method of Poly(vinylidene fluoride) (PVDF) Activated Carbon Air Cathodes for Microbial Fuel Cells, Environmental Science & Technology Letters 1 (2014) 416-420.
[26] M.M. Mardanpour, M. Nasr Esfahany, T. Behzad, R. Sedaqatvand, Single chamber microbial fuel cell with spiral anode for dairy wastewater treatment, Biosensors & bioelectronics 38 (2012) 264-269.
[27] A. Callegari, D. Cecconet, D. Molognoni, A.G. Capodaglio, Sustainable processing of dairy wastewater: Long-term pilot application of a bio-electrochemical system, Journal of Cleaner Production 189 (2018) 563-569.
[28] A. Faria, L. Gonçalves, J.M. Peixoto, L. Peixoto, A.G. Brito, G. Martins, Resources recovery in the dairy industry: bioelectricity production using a continuous microbial fuel cell, Journal of cleaner production 140 (2017) 971-976.
[29] Z. Chen, K. Li, P. Zhang, L. Pu, X. Zhang, Z. Fu, The performance of activated carbon treated with H3PO4 at 80° C in the air-cathode microbial fuel cell, Chemical Engineering Journal 259 (2015) 820-826.
[30] W. Yang, X. Wang, R. Rossi, B.E. Logan, Low-cost Fe–N–C catalyst derived from Fe (III)-chitosan hydrogel to enhance power production in microbial fuel cells, Chemical Engineering Journal 380 (2020) 122522.
[31] B.E. Logan, B. Hamelers, R. Rozendal, U. Schröder, J. Keller, S. Freguia, P. Aelterman, W. Verstraete, K. Rabaey, Microbial fuel cells: methodology and technology, Environmental science & technology 40 (2006) 5181-5192.
[32] Y. Yuan, S. Zhou, J. Tang, In situ investigation of cathode and local biofilm microenvironments reveals important roles of OH–and oxygen transport in microbial fuel cells, Environmental science & technology 47 (2013) 4911-4917.
[33] X. Zhang, S. Cheng, X. Wang, X. Huang, B.E. Logan, Separator characteristics for increasing performance of microbial fuel cells, Environmental science & technology 43 (2009) 8456-8461.
[34] O. Zimmo, N. Van der Steen, H.J. Gijzen, Comparison of ammonia volatilisation rates in algae and duckweed-based waste stabilisation ponds treating domestic wastewater, Water Research 37 (2003) 4587-4594.
[35] D. Fangueiro, M. Hjorth, F. Gioelli, Acidification of animal slurry–a review, Journal of environmental management 149 (2015) 46-56.
[36] M.J. Kampschreur, H. Temmink, R. Kleerebezem, M.S. Jetten, M.C. van Loosdrecht, Nitrous oxide emission during wastewater treatment, Water research 43 (2009) 4093-4103.
[37] T.H. Erguder, N. Boon, S.E. Vlaeminck, W. Verstraete, Partial nitrification achieved by pulse sulfide doses in a sequential batch reactor, Environmental science & technology 42 (2008) 8715-8720.
[38] G. Ruiz, D. Jeison, R. Chamy, Nitrification with high nitrite accumulation for the treatment of wastewater with high ammonia concentration, Water research 37 (2003) 1371-1377.
[39] S. Xin, J. Shen, G. Liu, Q. Chen, Z. Xiao, G. Zhang, Y. Xin, Electricity generation and microbial community of single-chamber microbial fuel cells in response to Cu2O nanoparticles/reduced graphene oxide as cathode catalyst, Chemical Engineering Journal 380 (2020) 122446.

[40] D. Clark, W. Feast, D. Kilcast, W. Musgrave, Applications of ESCA to polymer chemistry. III. Structures and bonding in homopolymers of ethylene and the fluoroethylenes and determination of the compositions of fluoro copolymers, Journal of Polymer Science: Polymer Chemistry Edition 11 (1973) 389-411.
[41] G.M. Burke, D.E. Wurster, M.J. Berg, P. Veng-Pedersen, D.D. Schottelius, Surface characterization of activated charcoal by X-ray photoelectron spectroscopy (XPS): correlation with phenobarbital adsorption data, Pharmaceutical research 9 (1992) 126-130.
[42] Y. Wu, X. Zhao, M. Jin, Y. Li, S. Li, F. Kong, J. Nan, A. Wang, Copper removal and microbial community analysis in single-chamber microbial fuel cell, Bioresource technology 253 (2018) 372-377.
[43] Y. Li, J. Liu, X. Chen, X. Yuan, N. Li, W. He, Y. Feng, Enhanced electricity generation and extracellular electron transfer by polydopamine–reduced graphene oxide (PDA–rGO) modification for high-performance anode in microbial fuel cell, Chemical Engineering Journal (2019) 123408.
[44] M. Li, S. Zhou, M. Xu, Graphene oxide supported magnesium oxide as an efficient cathode catalyst for power generation and wastewater treatment in single chamber microbial fuel cells, Chemical Engineering Journal 328 (2017) 106-116.
[45] S. Freguia, K. Rabaey, Z. Yuan, J. Keller, Non-catalyzed cathodic oxygen reduction at graphite granules in microbial fuel cells, Electrochimica Acta 53 (2007) 598-603.
[46] S.C. Popat, D. Ki, B.E. Rittmann, C.I. Torres, Importance of OH− transport from cathodes in microbial fuel cells, ChemSusChem 5 (2012) 1071-1079.
[47] S. Velasquez-Orta, I. Head, T. Curtis, K. Scott, Factors affecting current production in microbial fuel cells using different industrial wastewaters, Bioresource technology 102 (2011) 5105-5112.
[48] A.S. Mathuriya, V. Sharma, Bioelectricity production from various wastewaters through microbial fuel cell technology, Journal of Biochemical Technology 2 (2010) 133-137.
[49] S.V. Mohan, G. Mohanakrishna, G. Velvizhi, V.L. Babu, P. Sarma, Bio-catalyzed electrochemical treatment of real field dairy wastewater with simultaneous power generation, Biochemical Engineering Journal 51 (2010) 32-39.
[50] W. Yang, V.J. Watson, B.E. Logan, Substantial Humic Acid Adsorption to Activated Carbon Air Cathodes Produces a Small Reduction in Catalytic Activity, Environmental science & technology 50 (2016) 8904-8909.
[51] C. Lorinţ, M. Rădulescu, G. Buia, Influence of grazing practices on cow milk quality: a case study on the Comarnic–Poieni bauxite quarry, Romania, Environmental geochemistry and health 34 (2012) 289-295.
[52] W. Yang, R. Rossi, Y. Tian, K.-Y. Kim, B.E. Logan, Mitigating external and internal cathode fouling using a polymer bonded separator in microbial fuel cells, Bioresource technology (2017).
[53] J. An, N. Li, L. Wan, L. Zhou, Q. Du, T. Li, X. Wang, Electric field induced salt precipitation into activated carbon air-cathode causes power decay in microbial fuel cells, Water research 123 (2017) 369-377.
[54] B.E. Logan, M.J. Wallack, K.-Y. Kim, W. He, Y. Feng, P.E. Saikaly, Assessment of Microbial Fuel Cell Configurations and Power Densities, Environmental Science & Technology Letters 2 (2015) 206-214.

[55] X. Zhang, D. Pant, F. Zhang, J. Liu, W. He, B.E. Logan, Long‐term performance of chemically and physically modified activated carbons in air cathodes of microbial fuel cells, ChemElectroChem 1 (2014) 1859-1866.